$H_3PW_{12}O_{40}$ (PW_{12}) encapsulated on cotton-like mesoporous (CLM) silica as an efficient, reusable nano photocatalyst for the decolorization of Rhodamine B

R. Fazaeli*

Department of Chemistry, Shahreza Branch, Islamic Azad University, 86145-311, Iran.

Cotton-like mesoporous silica (CLM) was prepared by sol-gel technology. PW_{12}-containing cotton-like mesoporous silica system (PW_{12}@CLM) was studied with regard to its performance towards photodecolorization of Rhodamine B (RhB) dye solutions. The surface properties of the functionalized catalyst were analyzed by a series of characterization techniques like FTIR, XRD, N_2 adsorption–desorption, UV-vis and TEM. The photoefficiency of PW_{12}@CLM towards photodecolorization of RhB was investigated in a photocatalytic reactor using UV lamp as a light source.

Keywords: Supported photocatalyst; Encapsulation method; cotton-like mesoporous (CLM) silica; Rhodamine B.

INTRODUCTION

Azo dye containing waste water released into water bodies without decolorization is toxic to the ecosystem and also has significant influence on human health. Therefore, such pollutants have to be treated prior to discharging into the environment. They can be efficiently eliminated by photocatalytic decolorization, as an advanced oxidation process [1,2]. Rhodamine B (RhB) is a highly water soluble, basic red dye of the xanthene class. It is widely used as a colorant in textiles and food stuffs, and is also a well-known fluorescent water tracer. RhB is highly soluble in water and organic solvents, and its color is fluorescent bluish-red. This compound is now banned from use in foods and cosmetics because it has been found to be potentially toxic and carcinogenic. So the photodecolorization of RhB is important with regard to the purification of dye effluents [3,4]. Many catalysts such as $PbMoO_4$ [5], $MgFe_2O_4/TiO_2$ [6], TiO_2 bilayer films [7], TiO_2/AC [8] and $GdVO_4/g$-C_3N_4 [9] have been developed for degradation of RhB.

The photo-oxidation efficiency of POMs is comparable to that of the semiconductor TiO_2 [10-12]. Incorporation of $H_3PW_{12}O_{40}$ (PW_{12}) into a silica matrix to prepare insoluble POMs with mesoporous structure has been used in photocatalytic reactions [13-15].

It is well known that the size, morphology, and structure of mesoporous materials significantly influence their physical and chemical properties and, therefore, their applications [16]. Recently, much effort has been devoted to developing novel approaches for tailoring the structure of mesoporous materials to have specific morphologies, which is an important goal of material scientists. Studies have shown that combinations of various micelle interactions have led to the development of helical rods [17], helical fibers [18], shells [19], hollow or solid spheres [20,21], and faceted rhombododecahedra [22]. Based on this idea, a series of mesoporous materials with special morphologies, including solid spheres, hollow spheres and leaf shapes have been synthesized using different dual-template combinations [23-26].

The focus of the present work is to synthesize PW_{12}@CLM and apply it in the photodecolorization of RhB (C.I.No: 45170, formula weight=479.02, structure shown in Fig. 1), using UV irradiation. The effect of different parameters like initial dye concentration, catalyst loading, pH of the medium, temperature of the dye solution on the photodecolorization of RhB were studied in detail.
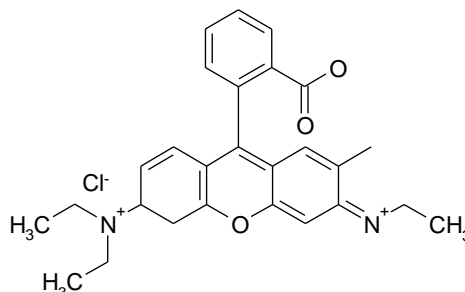

Fig. 1. Structure of Rhodamine B (RhB).

* To whom all correspondence should be sent:
E-mail: fazaeli@iaush.ac.ir

Preparation of CLM

LSM was synthesized using dodecylamine (DDA, 1.17 g) and F127 (0.5 g) as templates. The templates were dissolved in a mixture of ethanol (12 mL) and water (23 mL) under stirring for 30 min. TEOS (5 mL) was then added and the mixture was stirred for 24 h at ambient temperature. The solid product was recovered by filtration, then dried for 4 h at 110 °C and calcined for 4 h at 350 °C [27].

Preparation of PW₁₂@CLM

The supported PW_{12} catalyst was prepared under hydrothermal conditions. In a typical process, a 50 mg portion of PW_{12} was dissolved in deionized water and impregnated dropwise into 100 mg support (CLM) in 25 ml distilled water. The mixture was added to a Teflon container and kept under static conditions at 493 K for 8 h. The resulting solid was dried at 110 °C for 4 h and calcined at 350 °C for 4 h. According to elemental analysis, the loading was 27 wt% (Fig.2).
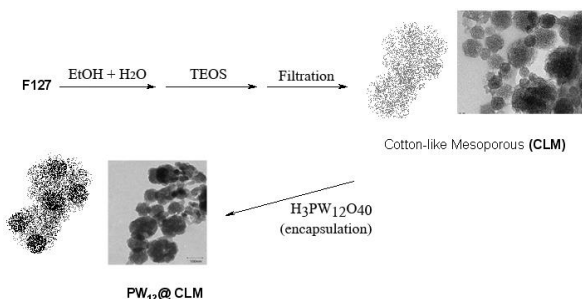

Fig. 2. Preparation of CLM and PW_{12}@CLM

RESULTS AND DISCUSSION

Physico-chemical characterization

The surface properties of PW_{12}@CLM were analyzed by a series of characterization techniques like FTIR, XRD, N₂ adsorption–desorption, UV-vis and TEM.
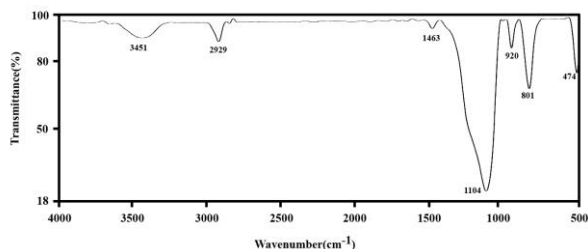

Fig. 3. FT-IR spectrum of PW_{12}@CLM.

FT-IR spectroscopy proved to be a powerful technique for studying the surface interaction between HPA and organic and inorganic supports.

Fig. 3 presents the FT-IR spectrum in the skeletal region of 4000–400 cm⁻¹ for the PW_{12}@CLM materials. In the spectrum of the parent CLM silica, a main band at 1090 cm⁻¹ with a shoulder at 1201 cm⁻¹ is observed that is due to asymmetric Si–O–Si stretching modes. Also, the corresponding symmetric stretching bands are observed at 812 and 961 cm⁻¹ [21]. The FT-IR spectrum of PW_{12}@CLM indicates that most of the characteristic bands of the parent Keggin structure, which could be found in the PW_{12} fingerprint region (1250–500 cm⁻¹), are not shown or appeared in the same assignable position of the bands corresponding to the ordered mesoporous silica host materials [28].

Fig.4 shows the XRD patterns of the parent CLM and PW_{12}@CLM in the low angle region (2θ = 0.6-8°). The main diffraction peak for CLM and PW_{12}@CLM is observed at 2θ=3.93 and 2θ=4.02, respectively. For PW_{12}@CLM systems, on low-angle X-ray diffraction, a slight shift of the primary peak to higher 2θ values, with a corresponding decrease in the peak intensity was also noted. The shift of the primary peak to higher scattering angles can be taken as an indication of a slight decrease in the sphere diameters, possibly due to a contraction of their frameworks with increasing PW_{12} loading during the calcination procedure. For PW_{12}@CLM, the intensities of the reflections decrease, indicating that the adopted synthesis procedure leads to less ordered materials than traditional CLM [29]. However, the arrangement of the CLM framework was still well retained after incorporation of PW_{12}, as can be seen from the TEM and N₂ adsorption data.
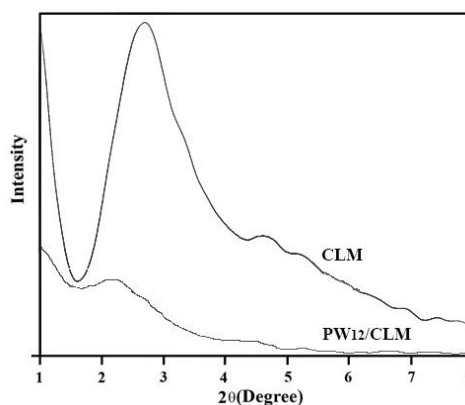

Fig.4. XRD patterns of CLM and PW_{12}@CLM.

The TEM image of the PW_{12}@CLM sample is shown in Fig. 5. The synthesized cotton-like mesoporous material clearly displayed a cotton shape and worm-like porous structure [27]. The same morphology was obtained for PW_{12}@CLM. TEM analyses indicate that the wrinkled porous structure of the CLM is robust enough to survive

the PW$_{12}$ incorporation process and so offers an excellent matrix to support highly dispersed PW$_{12}$ species. The places with darker contrast could be assigned to the presence of PW$_{12}$ particles with different dispersion. The small dark spots in the image could be ascribed to PW$_{12}$ particles, probably located in the PW$_{12}$@CLM cavities. The larger dark areas over the cavities most likely correspond to PW$_{12}$ agglomerates on the external surface.
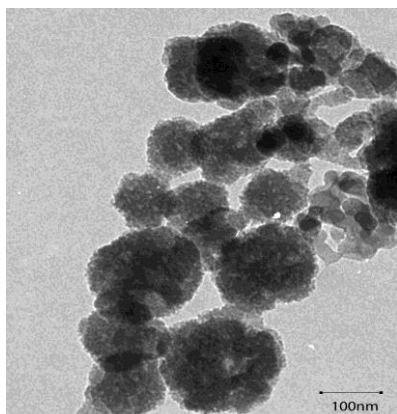

Fig. 5. TEM image of PW$_{12}$@CLM.

Structural properties of CLM and PW$_{12}$@CLM are listed in Table 1. CLM showed BET surface area of 1255 m^2/g and pore volume of 1.21 cm^3/g. After PW$_{12}$ modification, the nitrogen adsorption isotherm (Fig. 6) became an even line and the adsorbed volume decreased distinctly, suggesting the occupation of the pore by PW$_{12}$. BET surface area and pore volume of PW$_{12}$@CLM samples decreased which confirms that PW$_{12}$ has occupied the channels in CLM.

Two main absorptions are present in the DRUV–vis spectrum of pure PW$_{12}$: the first one is centered at 255 nm, and is attributed to the oxygen–tungsten charge-transfer absorption band for Keggin anions [30]. The second broad absorption in the PW$_{12}$ is centered at 360 nm with a shoulder at 345 nm. For PW$_{12}$@CLM (Fig. 7), these bands are clearly observed, and since pure nano-SiO$_2$ shows no UV absorption peak, therefore, these results indicated that a primary Keggin structure has been introduced into the nanostructure framework.
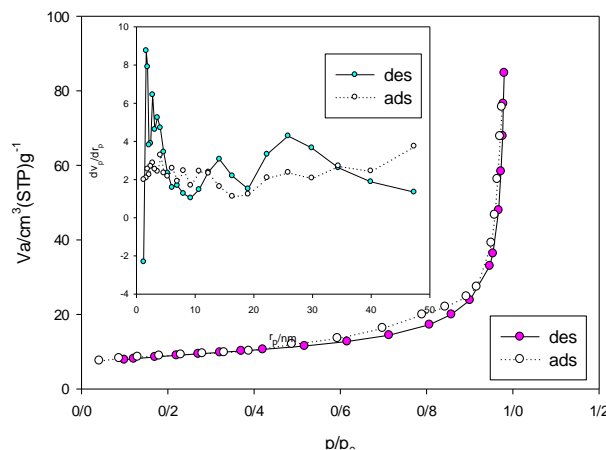
Fig. 6. N$_2$-adsorption-desorption isotherms of PW$_{12}$@CLM.
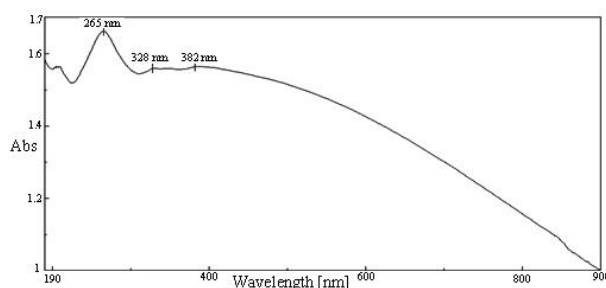
Fig. 7. DRUV–vis spectrum of PW$_{12}$@CLM.

Photocatalytic activity

After characterizing PW$_{12}$@CLM, the obtained material was used for the photocatalytic decolorization of a 40 ppm RhB dye solution containing 1 g L^{-1} photocatalyst under UV irradiation at varied conditions. A negligible decrease in the concentration of dye was observed under irradiation in the absence of photocatalyst or in the presence of photocatalyst without a light source. It is evident from the following results that the photolysis of the RhB solution in the presence of photocatalyst leads to the disappearance of the compound. In the absence of catalyst, direct photolysis of RhB was very slow and no appreciable photodecolorization, about 7 %, was observed during 60 min of UV irradiation, while in the presence of catalyst, the percentage of dye degraded after 60 min ranged from 7% to 92%.

Table 1. Texture parameters of CLM and PW$_{12}$@CLM samples.

| Material	Texture parameters (N$_2$ adsorption)		
	Surface area (m^2/g)	Pore volume (cm^3/g)^{a,b}	Pore diameter (nm)
CLM	1255	1.21	3.3
PW$_{12}$@CLM	380	0.96	1.8

^{a}Total pore volume measured at p/p$_0$ = 0.99.

^{b}Pore volume and pore size (by BJH method) determined from N$_2$ adsorption at 77K.

Effect of photocatalyst dosage

The effect of the amount of PW$_{12}$@CLM on the photodecolorization of RhB *versus* time is shown in Fig. 8a. It was observed that the decolorization percentage increased with increasing the amount of photocatalyst, reached the highest value (0.40 g L^{-1} of the photocatalyst) and then decreased. The reason for this decrease is thought to be the fact that when the concentration of the catalyst rises, the solid particles increasingly block the penetration of the photons.

So, the overall number of photons that can reach the catalyst particles and the production of OH radicals decrease with the loading of the catalyst. Another reason may be the decolorization of solid particles while using large amounts of catalyst [31].

a)
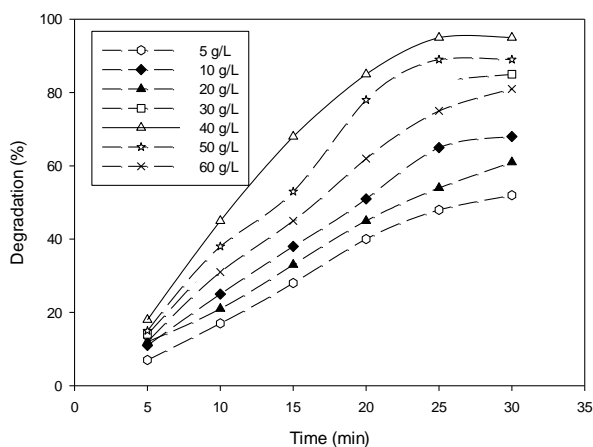
b)
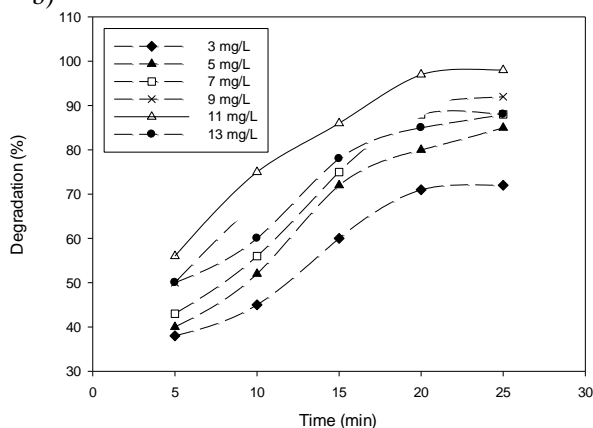
Fig. 8. (a) Effect of PW$_{12}$@CLM dosage on decolorization efficiency; initial RhB concentration, 11 mgL^{-1}; initial pH, 9; (b) Effect of initial dye concentration on RhB decolorization efficiency; 0.40 g L^{-1} of the catalyst; initial solution pH= 9.

Effect of the initial dye concentration

After optimizing the photocatalyst dosage, the effect of initial dye concentration ranging from 3 to 13 mg L^{-1} on the photodecolorization of RhB was investigated. The obtained results are shown in Fig.

8b. It can be seen that the rate of photodecolorization increases with increasing dye concentration up to 11 mg L^{-1}. This may be due to the fact that as the dye concentration was increased, more dye molecules were available for consecutive decolorization. The rate of photodecolorization was found to decrease with further increase in dye concentration, i.e., above 11 mgL^{-1}. The reason for this decrease is attributed to the shielding effect of the dye at high concentration that retards the penetration of light to the dye molecules deposited over the catalyst surface.
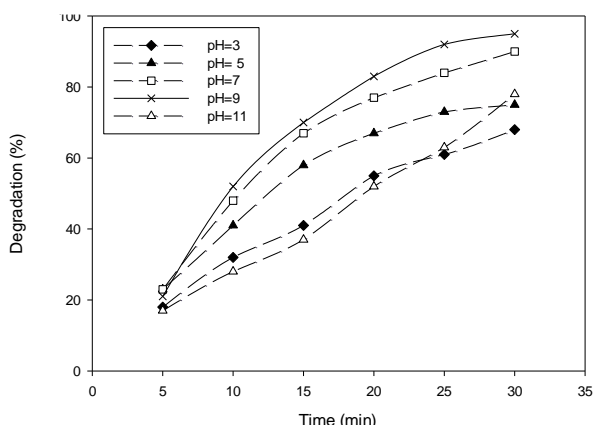
Influence of pH

The effect of pH in the range of 1-11 on RhB dye decolorization efficiency *versus* time is presented in Fig. 9. The pH value of the original solution of RhB is 9. Dilute hydrochloric acid solution or potassium hydroxide solution was used to tune the pH value when necessary. The initial concentration of RhB solution and dosage of the photocatalyst were kept at 11 mg.L^{-1} and 0.40 g.L^{-1}, respectively. Cationic dyes, such as RhB, undergo efficient degradation in the presence of PW$_{12}$@CLM under UV–Vis irradiation in alkaline media. These observations suggest that the charge characteristics of the dye substrates greatly influence their degradation. The effect of pH on the degradation of dyes in the presence of SiO$_2$ has been explained on the basis of point of zero charge (pH$_{pzc}$) of SiO$_2$ particles. The pH$_{pzc}$ of SiO$_2$ particles is 5.5 [32]. Thus, SiO$_2$ is positively charged in acidic solution (pH<5.5) and negatively charged in alkaline solution. According to this explanation and because of electrostatic interactions, cationic dyes (Rh.B) should be degraded at alkaline solution (Fig. 9). In alkaline solutions, the interaction between catalyst surface (Si–O-) and dye [specifically the nitrogen group, such as RhB, (Fig. 1)] favors the adsorption of the dye on the surface and accordingly, the photocatalytic activity increases [33].

Reusability of the catalyst

In our experiments, the stability and reusability of the photocatalyst were examined by repetitive use of the catalyst. After the dye was degraded in the first cycle, the photocatalyst was removed by filtration, washed several times with deionized water and dried at 90 and 350 °C for 2 h. This recovered catalyst was used again with the same concentration of RhB solution. The decomposition of RhB in the second cycle was almost as fast as in the first run. The fourth run of the decolorization of RhB showed no significant loss of photoactivity of

the catalyst, which indicated the considerable stability of the photocatalyst under the present conditions.

Fig. 9. Influence of solution pH on the RhB dye decolorization; 0.40 g L^{-1} of the catalyst; initial RhB concentration, 11 mgL^{-1}.

Comparison of PW$_{12}$@CLM with recently reported catalysts [5-9] for degradation of RhB shows that the photocatalytic activity of PW$_{12}$@CLM seems to be comparable with that of other known catalysts.

CONCLUSIONS

The results of this research demonstrated that PW$_{12}$@CLM is an efficient catalyst for the photodegredation of RhB. The results of the UV-Vis spectral changes indicate that the photocatalytic process can be used for complete decolorization and mineralization of RhB in the presence of PW$_{12}$@CLM in a photochemical reactor.

REFERENCES

1. C.G. Feng, X.X. Zhuo, X. Liu, *J. Rare Earths*, **25**, 717 (2009).
2. K. Bubacz, J. Choina, D. Dolat, A.W. Morawski, Polish. *J. Env. Stud.*, **19**, 685 (2010).
3. N. Barka, S. Qourzal, A. Assabbane, A. Nounah, Y. Ait-Ichou, *J. Photochem. Photobiol. A.*, **195**, 346 (2008).
4. L. You-ji, C. Wei, *Catal. Sci. Technol.*, **1**, 802 (2011).
5. D.B. Hernández-Uresti, J.A. Aguilar-Garib, A.M. la Cruz, *J. Microwave Power EE*, **46** (3), 163 (2012).
6. L. Zhang, Y. He, Y. Wu, T. Wu, Mater. *Sci. Eng. B.,* **176**, 1497 (2011).
7. J. Zhuang, W. Dai, Q. Tian, Z. Li, L. Xie, J. Wang, P. Liu, *Langmuir,* **26**(12), 9686 (2010).
8. Y. Li, S. Sun, M. Ma, Y. Ouyang, W. Yan, *Chem. Eng. J.*, **142**, 147 (2008).
9. Y. He, J. Cai, T. Li, Y. Wu, H. Lin, L. Zhao, M. Luo, *Chem. Eng. J., ***215–216**, 721 (2013).
10. A. Pearson, S. K. Bhargava, V. Bansal, *Langmuir*, **27**, 9245 (2011).
11. C. Yang, L. Tian, L.Ye, T. Peng, K. Deng, L. Zan, *J. Appl. Polymer Sci.,* **120**, 2048 (2011).
12. Z. Jiang, J. Han, X. Liu, *Adv. Mater. Res.,* **152-153**, 202 (2011).
13. Y.H. Guo , C.W. Hu , X.L. Wang ,Y.L. Wang , E.B. Wang ,Y.C. Zou , H. Ding , S.H. Feng. *Chem. Mater.*, **13**, 4058 (2001).
14. Y. Guo, Y. Wang, C. Hu. Y. Wang, E. Wang, Y. Zhou, S. Feng, *Chem. Mater.* **12**, 3501 (2000).
15. G. Marcì, E. García-López, M. Bellardita, F. Parisi, C. Colbeau-Justin, S. Sorgues, L. F. Liotta, L. Palmisano , *Phys. Chem. Chem. Phys.*, **15**,13329 (2013).
16. H.L. Xu, W.Z. Wang, *Angew. Chem. Int. Ed.* **46**, 1489 (2007).
17. S. Yang, L.Z. Zhao, C.Z. Yu, X.F. Zhou, J.W. Tang, P. Yuan, D.Y. Chen, D.Y. Zhao, *J. Am. Chem. Soc.* **128**, 10460 (2006).
18. G.L. Lin, Y.H. Tasi, H.P. Lin, C.Y. Tang, C.Y. Lin, *Langmuir*, **23**, 4115 (2007).
19. Y.Q. Yeh, B.C. Chen, H.P. Lin, C.Y. Tang, *Langmuir*, **22**, 6 (2006).
20. Y.F. Zhu, J.L. Shi, H.R. Chen, W.H. Shen, X.P. Dong, *Micropor. Mesopor. Mat.*, **85**, 75 (2005).
21. W.Q. Wang, J.G. Wang, P.C. Sun, D.T. Ding, T.H. Chen, *J. Colloid Interf. Sci.* **331**, 156 (2009).
22. B.C. Chen, M.C. Chao, H.P. Lin, C.Y. Mou, *Micropor Mesopor Mat.*, **81**, 241 (2005).
23. J.G. Wang, F. Li, H.J. Zhou, P.C. Sun, D.T. Ding, T.H. Chen, *Chem. Mater.,* **21**, 612 (2009).
24. H. Blas, M. Save, P. Pasetto, C. Boissiere, C. Sanchez, B. Charleux, *Langmuir*, **24**, 13132 (2008).
25. Z. Feng, Y.S. Li, D.C. Niu, L. Li, W.R. Zhao, H.R. Chen, L. Lei, J.H. Gao, M.L. Ruan, J.L. Shi, *Chem. Commun.*, 2629 (2008).
26. F. Cavani, N. Ballarini, A. Cericola, *Catal. Today*, **127**, 113 (2007).
27. L.Du, H. Song, S. Liao, *Appl. Sur. Sci.* **255**, 936 (2009).
28. R. Fazaeli, H. Aliyan, S. Parishani Foroushani, Z. Mohagheghian*, Turk. J. Chem.*, **38**, 372 (2014).
29. R. Fazaeli, H. Aliyan, E. Naderi, *Phosphorus, Sulfur*, **188**, 745 (2013).
30. J. Juan-Alcaniz, E. V. Ramos-Fernandez, U. Lafont, J. Gascon, F. Kapteijn, *J. Catal.*, **269** 229 (2010).
31. H. Aliyan, R. Fazaeli, R. Jalilian, *Appl. Sur. Sci.*, **276**, 147 (2013).
32. M. Guedes, J.A.F. Ferreira, A.C. Ferro, *J. Colloid Inter. Sci.* **337**, 439 (2009).
33. H. Aliyan, R. Fazaeli, R. Jalilian, *Appl. Sur. Sci.*, **276**, 147 (2013).

H₃PW₁₂O₄₀ (PW₁₂) КАПСУЛИРАН В ПАМУКО-ПОДОБЕН МЕЗОПОРЬОЗЕН СИЛИЦИЕВ ДИОКСИД (CLM) КАТО ЕФЕКТИВЕН И МНОГОКРАТНО УПОТРЕБЯВАН НАНО-ФОТОКАТАЛИЗАТОР ЗА ОБЕЗЦВЕТЯВАНЕТО НА RHODAMINE B

Р. Фазаели

Департамент по химия, Клон Шахреза, Ислямски университет „Азад", 86145-311, Иран

(Резюме)

Приготвен е памуко-подобен мезопорьозен силииев диоксид (CLM) по зол-гел технология. Изследвана е PW₁₂-съдържаща система с памуко-подобен мезопорьозен силииев диоксид (PW₁₂@CLM) по отношение на фото-химичното обезцветяване на Rhodamine B (RhB) в багрилни разтвори. Повърхностните свойства на този катализатор са анализирани с различни техники, като FTIR, XRD, N₂ адсорбция/десорбция, UV-Vis и TEM. Ефективността спрямо PW₁₂@CLM фото-обзцветяването на RhB е изследвана във фото-каталитичен реактор с UV-лампа като светлинен източник.